Available online at www.sciencedirect.com
ScienceDirect
Thermochimica Acta 450 (2006) 118–125
thermochimica acta
www.elsevier.com/locate/tca

Sorption isotherms, sorption enthalpies, diffusion coefficients and permeabilities of water in a multilayer PEO/PAA polymer film using the quartz crystal microbalance/heat conduction calorimeter

Allan L. Smith [a,*], J. Nathan Ashcraft [a], Paula T. Hammond [b]

[a] *Masscal Corporation, 96 A. Leonard Way, Chatham, MA 02633, United States*
[b] *Department of Chemical Engineering, MIT, Cambridge, MA 02139, United States*

Available online 28 September 2006

Abstract

Sorption isotherms, sorption enthalpies, and diffusion coefficients for water in an 11 μm thick PEO/PAA multi-layer film have been measured at 30, 40, and 60 °C for relative humidities between 0 and 70%. All quantities were measured on the same film using the quartz crystal microbalance/heat conduction calorimeter. Water diffusion coefficients in the film are several orders of magnitude lower than in the separate components. Sorption isotherms are of type III at 30 and 40 °C and linear at 60 °C. Water vapor permeabilities are calculated as the product of Henry's law solubility and diffusion coefficient. The permeability of the PEO/PAA multilayer film is exceedingly low compared to other polymer films used as membranes. The enthalpy of water sorption determined from the sorption isotherms using the van't Hoff relation is 32.9 ± 0.3 kJ/mol. Calorimetric enthalpies of water sorption range from 42 to 34 kJ/mol at 30 and 40 °C over the humidity range studied. The change in motional resistance, a quantity proportion to the loss compliance of the film, has also been recorded at all three temperatures, and a common trend is an increase in loss compliance with increasing relative humidity, indicating plasticization of the film by water.

Keywords: Layer-by-layer film; Water sorption; Quartz crystal microbalance/heat conduction calorimetry; Poly(ethylene oxide); Poly(acrylic acid); Sorption isotherm; Water diffusion coefficient; Permeabililty

1. Introduction

The measurement and control of water permeability in polymer films and membranes is important in many industrial applications: membranes for fuel cells and gas separation [1,2], high performance electronic coatings, packaging, drug delivery systems, and contact lenses [3], to name a few. In particular, water management is critical in proton exchange membrane (PEM) fuel cells to ensure operation in an optimally humidified environment, but where flooding of the electrodes is prevented.

Water transport in a fuel cell membrane occurs by electro-osmotic drag from the anode to cathode (as current is drawn) and by back diffusion from the cathode to anode (as water is produced) because of the difference in water concentration between the electrodes. However, the inlet gases are also usually humidified to ensure operating conditions where the PEM will have high ionic conductivity values. For example, standard PEMs such as Nafion® require fuel cell operating conditions of least 80% RH for acceptable performance [4–6]. An understanding of the water transport properties of a PEM is therefore important in optimizing fuel cell performance and potentially reducing the complexity of the overall fuel cell system. It would also be desirable to have to capability to tune the water transport properties of a PEM to improve the performance and stability of the membrane. Fuel cells that can operate over a wider humidity range are desirable, especially for portable applications where additional water management systems are not practical.

Recent work by Hammond and Farhat [7] has shown that PEMs constructed by the layer-by-layer (LBL) assembly technique can perform comparably or even better than Nafion® systems at lower humidities (<60% RH). The best performing PEM from that study, a thin film composed of poly(ethylene oxide) and poly(acrylic acid), will be examined here for its water sorption properties.

The behavior of both inorganic and organic thin films and coatings is influenced by the presence of moisture retained from

* Corresponding author. Tel.: +1 508 241 8628; fax: +1 508 348 0303.
E-mail address: asmith@masscal.com (A.L. Smith).

0040-6031/$ – see front matter © 2006 Elsevier B.V. All rights reserved.
doi:10.1016/j.tca.2006.09.011

the original drying and curing process or moisture absorbed from the surroundings while the product is stored or in use. The most common property used to quantify moisture sorption [8] is permeability, P, defined as the product of the solubility S and the diffusion coefficient D:

$$P = S \times D \quad (1)$$

The solubility of gases in polymers is an equilibrium thermodynamic property—the slope of the sorption isotherm (mass fraction or volume fraction of vapor sorbed versus partial pressure) and is normally measured with a static gravimetric technique. The diffusion coefficient is a dynamic property, the proportionality constant relating flux and concentration gradient, and it is measured with both steady state and time-dependent techniques that differ from those used for solubility.

Another important thermodynamic property characterizing water–polymer interactions is the water sorption enthalpy. With few exceptions, this enthalpy has been determined for polymers from the van't Hoff equation relating Henry's law solubility and temperature. Direct calorimetric determination of enthalpies of water sorption is tedious because of the slowness of the sorption process in bulk polymers.

We show here that it is possible to measure the solubility and the diffusion coefficient (and thus the permeability), as well as the enthalpy of water sorption in a thin polymer film applied to the surface of a quartz crystal microbalance (QCM). By combining this QCM with a heat conduction calorimeter (HCC), we show that it is also possible to measure the water sorption enthalpy [9] and the plasticizing effect of solvent sorption [10]. In this work, we use the Masscal G1 QCM/HCC to measure these four quantities in a composite poly(ethylene oxide)/poly(acrylic acid) film prepared by the LBL technique.

2. Experimental

2.1. Preparation of the film

Poly(ethylene oxide) (PEO, $M_w = 4{,}000{,}000$) and poly(acrylic acid) (PAA, $M_w = 90{,}000$) were from Polysciences, Inc. and used as received; 1,1-mercaptoundecanoic acid (MUA) was from Aldrich. QCM crystals having a surface area of 5.067 cm^2 were from Masscal Corporation. The QCM crystals were cleaned by ultrasonication in a Cole-Parmer 8848 bath. Subsequently, the crystals were rinsed in a series of ethanol and water several times, dried under nitrogen, and then plasma-etched for 3 min. Clean crystals were placed in 0.01 M MUA (dissolved in ethanol) for 2 h. to functionalize the surface.

PEO and PAA were dissolved in Millipore MilliQ filtered water (18.2 MΩ cm) to yield 0.02 M (based on repeat unit of the polymers) solutions, and aqueous HCl was used to adjust the pH of all solutions to 2.5. Prior to film construction the back of the QCM crystals were protected with tape, and then films were deposited on the functionalized QCM crystals.

Film deposition occurred by use of a programmable ZEISS DS50 slide stainer. The substrate was first immersed in the PEO solution for 10 min, followed by three 2 min rinses in pH 2.5 water baths to remove any loosely bound polymer. The substrate with adsorbed PEO was then submerged in the PAA solution for 10 min, followed by the same three step rinsing procedure. The process was then repeated 90 times to produce a film of "90 bilayers" and dried under nitrogen at the end of fabrication. After drying, the tape was removed, and the back of the crystal was cleaned with acetone to remove any tape residue. The mass of film adsorbed was determined by comparing the mass of the crystal before and after deposition.

The mass of the PEO/PAA film coated on the QCM crystal was 7.5 mg. From the Sauerbrey equation [11] and the observed frequency shift between coated and bare QCM, the film mass was computed to be 6.71 mg for an area of 5.067 cm^2, the total area of one side of the crystal. This 12% difference between the two measurements of film mass is understandable, since the film was somewhat non-uniform over the crystal surface and the QCM calculation assumes uniform mass distribution. Assuming a density of 1.2 g/cm^3 for the film, the film thickness is computed to be 11.0 μm.

2.2. The apparatus

The operating principles of the quartz crystal microbalance/heat conduction calorimeter have been presented elsewhere [11]. Here we summarize the Masscal G1 performance specifications relevant to these experiments. The temperature of the sample chamber containing the mass/heat flow sensor is controllable from several degrees above ambient to 100 °C, to ±0.004 °C. Humidified nitrogen from an external relative humidity generator flows through the chamber at 10 cm^3 (STP)/min. Measured baseline stabilities (standard deviations) in a 7 h period are: mass per unit area, ±0.001 μg/cm^2; thermal power, ±230 nW; motional resistance, ±0.02 Ω. The thermal time constant of the calorimeter is 12 s, comparable to the residence time of the gas in the sample chamber. A program of variable relative humidity versus time, generated by the G1 Control software, is achieved by mixing a dry N_2 stream and a fully humidified stream generated by two mass flow controllers [11]. Achievable relative humidities are 0–70%, with the water bubbler at ambient laboratory temperature, 25 °C. The relative humidity of the output gas stream at the ambient laboratory temperature is measured in real time using a Sable Systems RH200 RH/dewpoint analyzer.

3. Results and analysis

The coated QCM was taken from the ambient lab atmosphere and placed in the G1 at 30° with a stream of dry air flowing over its surface at 10 cm^3(STP)/min. Fig. 1 shows the three signals – mass per unit area, heat flow, and motional resistance – collected as the film dried slowly over the next four hours. Most mass loss occurs in the first hour.

Seven runs were taken on the PEO/PAA film. Details are summarized in Table 1.

Fig. 2 shows the data collected in run 30A. Notice that the relative humidity reaches steady-state ∼200 s after the step-change,

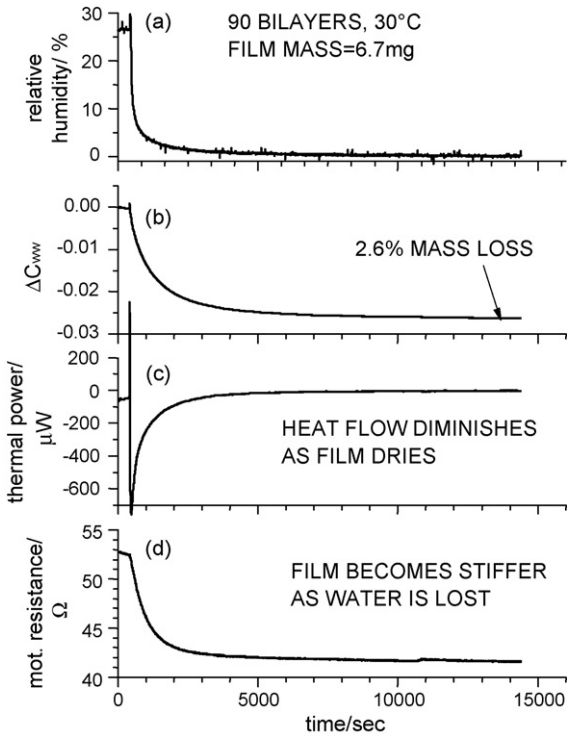

Fig. 1. QCM/HCC data from the drying of an 11 μm 90 bilayer PEO/PAA film at 30 °C. (a) Relative humidity at sample chamber output (%). (b) Change in weight concentration (gH_2O/g of polymer). (c) Thermal power (μW). Negative is heat flow from sample. (d) Motional resistance of sample and QCM (Ω).

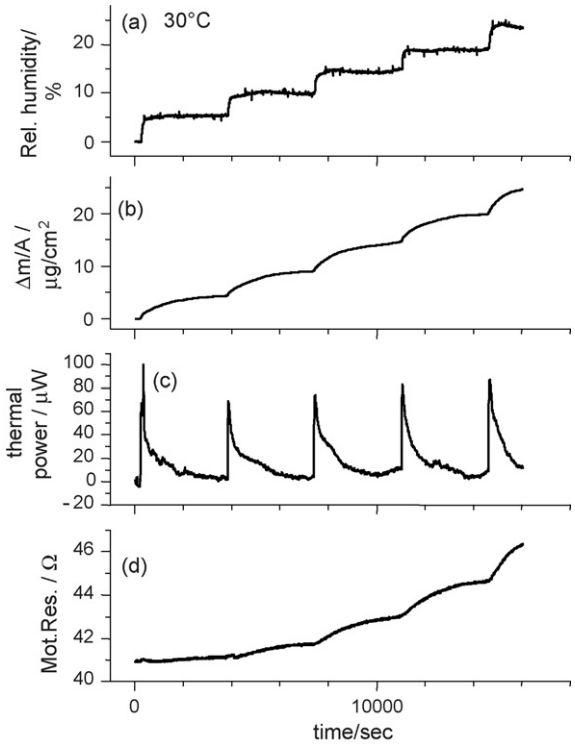

Fig. 2. QCM/HCC collected when the PEO/PAA film is exposed to 1-h stepwise changes in relative humidity at 30 °C. Dataset 30A. (a) Relative humidity. (b) Change in mass per unit area of the sample (μg/cm^2). (c) Thermal power. Positive is heat flow to sample. (d) Motional resistance of sample and QCM.

whereas the response signals from the film take several thousand seconds to equilibrate. The delay is caused by slow diffusion of water into the film.

3.1. Diffusion coefficients

Hernandez-Munos and Gavana have shown [12] that if the mass $m(t)$ of a uniform polymer film of thickness l deposited on a non-absorbing substrate is measured continuously as the partial pressure of an absorbing species in contact with that film is varied in a stepwise manner, then the diffusion coefficient of the species can be calculated. The working equation for data analysis is

$$\frac{-1}{\pi^2} \ln\left(\frac{(m_p^\infty - m_p^t)\pi^2}{8(m_p^\infty - m_p^i)}\right) = \frac{D}{l^2}t \quad (2)$$

Here m_p^t is the mass of the film plus sorbate taken up at any time t, m_p^i the corresponding mass at the beginning of analysis, m_p^∞ the mass at steady state, D the diffusion coefficient, l the film thickness, and t is the time. This equation applies within 0.1% for a sorption range of 35–85%.

The dataset at 60 °C shows that diffusion is fast enough for the mass signal to follow the relative humidity change closely, so Eq. (2) is not applicable. However, at lower temperatures the delay is long enough to determine diffusion coefficients by using Eq. (2). Table 2 contains these diffusion coefficients determined at various relative humidities for water vapor in the PEO/PAA multilayer film at 30 and 40 °C; the data are plotted in Fig. 3. Also shown are quadratic fits to the data, the coefficients and statistics of which are in Table 3.

Table 1
Masscal G1 data files analyzed in this work

Run	Description
30 dry	30 °C. Overnight run. First 7 min, ambient air; remainder, dry N_2
30A	30 °C. After a short 0% RH baseline, five 1-h steps 5–10–15–20–25% RH
30B	30 °C. Overnight run. One-hour steps 0–20–40–20–0% RH
30C	30 °C. Four 1-h steps 40–50–60–70% RH
40A	40 °C. Six 1-h steps 0–5–10–15–20–25% RH
40B	40 °C. Six 1-h steps 25–30–35–40–45–50% RH
60	60 °C. Six 1-h steps 0–5–10–15–20–25% RH

3.2. Sorption isotherms

From the mass and relative humidity data we determined the water vapor sorption isotherms for each run – gravimetrically defined solubility (the mass of water absorbed per unit mass of polymer film), as a function of the relative humidity. Following the notation conventions of Paterson et al. [13], the working

Table 2
Diffusion coefficients and sorption isotherms for H_2O in PEO/PAA

RH (%)	Diffusion coefficient (cm^2/s)	C_{ww}[a]
Runs 30B and 30C		
0		0.0000
20	1.030E−10	0.0185
40	2.410E−10	0.0388
50	3.127E−10	0.0531
60	4.894E−10	0.0698
70	4.311E−10	0.0901
Run 30A		
0		0.0000
5	1.13E−10	0.0033
10	1.19E−10	0.0069
15	1.02E−10	0.0112
20	1.12E−10	0.0153
25	1.87E−10	0.0194
Runs 40A and 40B		
0		0.0000
5	1.25E−10	0.0024
10	1.80E−10	0.0049
15	2.29E−10	0.0074
20	2.14E−10	0.0100
25	1.99E−10	0.0128
30	2.84E−10	0.0160
35	3.54E−10	0.0191
40	2.60E−10	0.0227
45	4.85E−10	0.0258
50	4.76E−10	0.0293
Run 60		
0		0.0000
5	4.69E−10	0.0011
10	1.58E−09	0.0019
15	2.52E−09	0.0027
20	2.34E−09	0.0034
25	8.94E−10	0.0044

[a] Units of C_{ww} are gH_2O/g film.

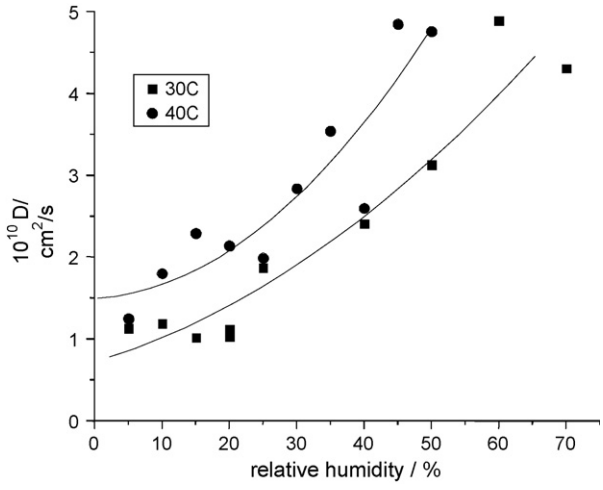

Fig. 3. Diffusion coefficients of water (cm^2/s) in the PEO/PAA multilayer film at 30 and 40 °C.

Table 3
Quadratic fits to diffusion coefficient vs. relative humidity, $D = A + B_1RH + B_2RH^2$

T (°C)	A	B_1	B_2	R^2	S.D.
30	7.23E−11	2.40E−12	5.01E−14	0.916	4.7E−11
40	1.50E−10	4.51E−13	1.23E−13	0.840	5.5E−11

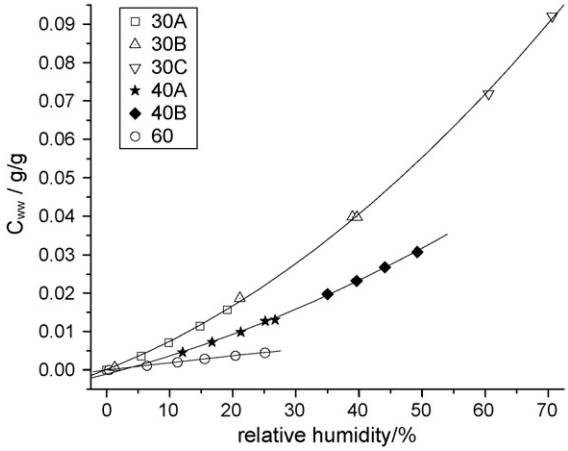

Fig. 4. Water vapor sorption isotherms (C_{ww} vs. relative humidity) in the PEO/PAA film at 30, 40, and 60 °C. See Table 1 for details of each run.

equation for solubility is

$$C_{ww} = \frac{\Delta m/A_{run}}{\Delta m/A_{film}} \quad (3)$$

where $\Delta m/A_{run}$ is the change in mass per unit area of a given run and $\Delta m/A_{film}$ is the mass per unit area of the dry film (in this case, 1275 $\mu g/cm^2$). Fig. 4 shows these data along with quadratic fits for each temperature. Table 4 contains coefficients and the statistics for each fit.

3.3. Sorption enthalpies

The thermal power signal $P(t)$ due to the sorption of water vapor by a thin film adhering to the surface of the QCM has been shown [14] to be proportional to the rate of change of mass signal:

$$P(t) = \frac{dQ}{dt} = \frac{\Delta H}{M}\frac{dm}{dt} \quad (4)$$

where ΔH is the enthalpy of sorption of water vapor in the film and M is the molar mass of water. Integration of both sides yields

Table 4
Quadratic fits to sorption isotherms, $C_{ww} = A + B_1RH + B_2RH^2$

T (°C)	A	B_1	B_2	R^2	S.D.
30	3.302E−6	6.464E−4	9.148E−6	0.99953	6.33E−4
40	−0.00111	4.234E−4	4.638E−6	0.99932	2.69E−4
60	−1.086E−4	2.000E−4	−6.538E−7	0.99943	5.12E−5

an equation for ΔH at any time during the run:

$$\Delta H(t) = \frac{MQt}{m(t)} \tag{5}$$

Because each data file contains real-time measurements of all relevant quantities in Eqs. (4) and (5), it is possible to plot what we shall call the "running enthalpy of sorption" $\Delta H(t)$ versus time for each run. Corrections must be made to the thermal power signal $P(t)$ before its indefinite integral $Q(t)$ is evaluated. There are three contributions to the measured thermal power: the heat flow generated by the sample itself P_{sam}, the thermal power generated by the QCM when driven by the RF electronics that excites it, and the spurious thermal power sometimes observed from the sample chamber with a bare, uncoated crystal, P_{chamber}:

$$P_{\text{tot}} = P_{\text{sam}} + P_{\text{cryst}} + P_{\text{chamber}} \tag{6}$$

Recent improvements in the design of the mass/heat flow sensor and sample chamber assembly in the G1 have reduced the contribution of the spurious thermal power to less than 1% of the large signals observed here; details will be described elsewhere. The power generated in the QCM crystal depends on the motional resistance of the crystal, as given by a relationship obtained from the manufacture of the RF electronics subcomponent:

$$P_{\text{cryst}} = \frac{10^6\, R_{\text{m}}}{32(R_{\text{m}} + 62.5)^2} \tag{7}$$

where R_{m} is the motional resistance in ohms. Typical steady-state values for this term are 50–100 μW, and the changes in motional resistance caused by sorbed water vapor may produce 5–10 μW changes in P_{cryst}. P_{sam} is calculated before the integrated heat $Q(t)$ is obtained from Eq. (6).

If the film is in true equilibrium with the water vapor towards the end of the equilibration period, then $\Delta H(t)$ should become independent of time during this period. Fig. 5 shows the running enthalpy of sorption $\Delta H(t)$, the integrated heat $Q(t)$, the thermal power of the sample $P_{\text{sam}}(t)$, the change in mass per unit area produced by water sorption $\Delta m/A(t)$, and the relative humidity program RH(t) for run 40B. Notice that although the signals Q and $\Delta m/A$ track each other closely, their ratio ΔH is not constant but varies by about 10%. Several subtle effects contribute to this variation; we believe the major contribution is to a slowly drifting thermal power baseline. Earlier runs (30A and 60) were taken on a different Masscal G1 with a larger contribution from the spurious thermal power signal. We included only the files 30B, 30C, 40A, and 40 B in this analysis. Fig. 6 shows values of $\Delta H(t)$ determined 600 s before each step change in relative humidity for these four runs. We estimate errors of ±10% for a given ΔH.

3.4. Plasticization of the film by sorbed water

We have shown [10] that the difference in motional resistance of a coated and uncoated QCM crystal is proportional to the loss compliance of the coating:

$$\Delta R = \frac{2L_{\text{q}}}{3\pi Z_{\text{q}}}\omega^4 \rho_{\text{f}}^2 h_{\text{f}}^3 J'', \tag{8}$$

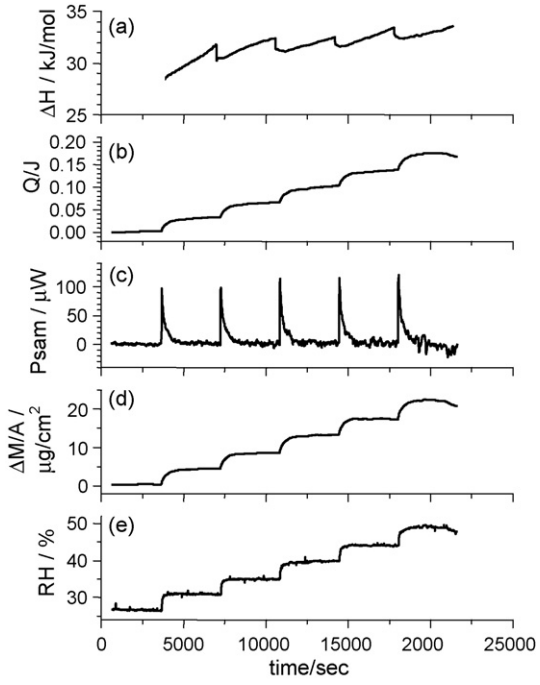

Fig. 5. Running enthalpy of water vapor sorption (kJ/mol) in PEO/PAA film at 40 °C. Run 40B.

and that the increase in loss compliance that occurs when the coating absorbs a volatile organic solvent or water is a quantitative measure of the plasticization of the film by that solvent. In Eq. (8) L_{q} and Z_{q} are the properties (the inductance and motional impedance) of the 5 MHz quartz crystal, ω the angular frequency of oscillation, h_{f} the film density, h_{f} the film thickness, and J'' is the film loss compliance. At 0% relative humidity and 30 °C the motional resistance is 41 Ω, while for the uncoated crystal it was 9 Ω. From Eq. (5) we calculate a loss compliance at 5 MHz of 1.8×10^{-11} Pa^{-1} for the PEO/PAA film. By comparison, the loss compliance several other polymers at 5 MHz is given in Table 5.

The data of Fig. 2 show that the motional resistance, and thus the loss compliance increases with increasing relative humidity,

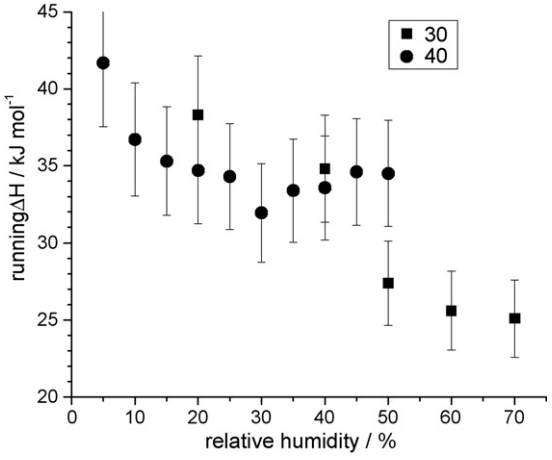

Fig. 6. Water vapor sorption enthalpies (kJ/mol) in the PEO/PAA film at 30 and 40 °C for various relative humidities.

Table 5
Loss compliance of some polymeric materials at 5 MHz

Material	Loss compliance at 5 MHz and room temperature (Pa^{-1})	Reference
Poly(*n*-butyl acrylate)	5×10^{-9}	[21]
Polyisobutylene rubber	2.4×10^{-9}	[22]
Polystyrene	2×10^{-13}	[23]
Decrolon spray enamel	2.5×10^{-9}	[10]
PEO/PAA multilayer film	1.8×10^{-11}	This work

as is expected. An increase from 0 to 25% relative humidity produces a 19% increase in loss compliance. The runs in Table 1 contain useful information on the plasticizing effect of water vapor on the PEO/PAA film; detailed analysis will be presented elsewhere.

4. Discussion

4.1. Diffusion coefficients

Fig. 3 shows that the diffusion coefficients at 40 °C are larger than those at 30 °C. This is expected from the expected van't Hoff–Arrhenius form for the temperature dependence of D [8]:

$$D(T) = D_0 \exp\left(-\frac{E_D}{RT}\right) \quad (9)$$

From the quadratic fits in Table 3 we calculate the activation energy E_D for the diffusion coefficient to decrease from 55 kJ/mol at 0% RH to 30 kJ/mol at 50% RH. The diffusion coefficient data in Fig. 3 have a large scatter, so the activation energies are only approximate.

The diffusion coefficients reported here are two orders of magnitude less than water diffusion coefficients in PAA and in amorphous PEO. In Table 3 of Prausnitz et al. [15] the water diffusion coefficient at 35 °C is given as 0.98×10^{-8} cm^2 s^{-1} at a relative humidity of 58%. Elberaichi et al. [16] report the diffusion coefficient of water in amorphous PEO at 20 °C to be 6×10^{-7} cm^2 s^{-1}.

4.2. Sorption isotherms and solubility

Fig. 4 shows that the sorption isotherms for 30 and 40 °C are linear at low relative humidity and then curve upward, as is typical of a type III sorption isotherm of the Flory–Huggins model [8]. Water sorption in polymers has often been analyzed using this model, particularly if the interest is in polymer-water interactions at higher water vapor activity [17]. Here we focus on the region of low water vapor activity, where Henry's law behavior applies and the sorption isotherm is linear with relative humidity. We adopt van Krevelen's definition of solubility as the amount of gas per unit volume of polymer in equilibrium with a unit partial pressure, as expressed in the equation:

$$C_{ww} = \mathrm{Sp}\,(\text{Henry's law}) \quad (10)$$

where the units of S are cm^3 (STP)/cm^3 of polymer per bar. The linear terms in the sorption isotherm equation (Table 4) was used to compute the Henry's law solubility S of water vapor in the PEO/PAA film at the three temperatures. The results are given in Table 6. Also given in Table 6 are the permeabilities of water in the film. The unit of permeability is the barrer: 1 barrer = 10^{-10} cm^3 (STP) cm/cm^2 s cmHg.

Comparison of the sorption isotherms measured here with those in similar systems is instructive. Van Krevelen [8] has tabulated the molar water content per structural group of various polymers at different relative humidites at 25 °C. Using the data of his Table 18.11, we estimate the concentration C_{ww} of water (gH_2O/g polymer) in PAA at 25 °C for various humidities and compare it with PEO/PAA in Table 7. For this calculation, the oxygen-containing functional group in PAA is assumed to be neutral –COOH because the PEO/PAA film was prepared at pH 2.5. These results suggest that water is absorbed predominantly by the PAA component in the multilayer film.

Two prior studies of water sorption in PAA are relevant here. Chang, Myerson, and Kwei [18] reported equilibrium (Henry's law) sorption isotherms for water vapor in PAA at 40 °C. From their Fig. 4, C_{ww} at 38% RH is .0095 g H_2O/g polymer. Prausnitz et al. [15] measured sorption isotherms for water vapor in PAA at 35 °C. The lowest value of relative humidity in their data was 29%, for which C_{ww} was 0.0384 g H_2O/g polymer. From the

Table 6
Henry's law solubility and permeability of water in PEO/PAA film

T (°C)	S (cm^3 (STP)/cm^3 polymer bar)	D (cm^2/s)[a]	P (barrer)
30	2110	$1.3 \pm 0.3 \times 10^{-11}$	36
40	1390	$2.1 \pm 0.4 \times 10^{-11}$	38
60	654	$1.6 \pm 0.9 \times 10^{-10}$	140

[a] Diffusion coefficients were averaged over the range of 0–25% RH for all temperatures.

Table 7
Water concentration C_{ww} in PAA and PEO/PAA for various relative humidities

Polymer	C_{ww} (30% RH)	C_{ww} (50% RH)	C_{ww} (70% RH)	Reference
PAA	0.05	0.075	0.15	[8], 25 °C
PEO/PAA	0.0276	0.0552	0.0901	This work, 30 °C

results in this work, at 29% RH, $C_{ww} = 0.0264\,gH_2O/g$ film at 30 °C and .0151 gH_2O/g film at 40 °C. The surprising result here is that the layer-by-layer addition of a very hydrophilic, water-soluble poly(ethylene oxide) [19] to poly(acrylic acid) actually decrease the solubility.

4.3. Calorimetric sorption enthalpies and van't Hoff sorption enthalpies

From the data of Fig. 6 we conclude that the calorimetric enthalpy of water vapor sorption in the PEO/PAA film at 40 °C decreases from 42 kJ/mol at low humidities to 34 kJ/mol at 50% RH, and that the sorption enthalpy at 30 °C is somewhat lower, particularly at high RH.

The usual method used to estimate vapor sorption enthalpies in polymers is van't Hoff analysis. The Henry's law solubility S is assumed to have a temperature dependence comparable to other solid–gas equilibria:

$$S = S_0 \exp\left(\frac{-\Delta H_s}{RT}\right) \tag{11}$$

where ΔH_s is the van't Hoff enthalpy of sorption of the vapor in the polymer. Although there is no thermodynamic reason to assume that this equation is valid for a two-component system such as the PEO/PAA film, it is still of interest to derive a van't Hoff enthalpy of water sorption from the Henry's law equilibrium solubilities $S(T)$ by fitting the equation:

$$\ln(S(t)) = \frac{\ln(S_0) - \Delta H_s}{RT} \tag{12}$$

From the data in Table 6 we calculate $\Delta H_s = 32.8$ kJ/mole, with a standard deviation from the fit of less than 1%, in good agreement with the calorimetrically determined enthalpies of water vapor sorption in PEO/PAA.

4.4. Permeabilities

Wessling et al. [20] have reviewed the transport of water vapor and inert gas mixtures through highly selective and highly permeable polymer membranes. The most frequently used method of measuring permeabilities is the cup method. This method consists of a polymeric film covering a container with water or a desiccant. The container is placed in a humidity-controlled environment, and the permeability of water vapor through a polymeric film is determined by the rate of weight decrease of the container. More accurate results can be obtained with the variable-pressure constant-volume method, where a vacuum is applied at the permeate side of the membrane and water vapor is present at the feed side of the membrane. The water permeability is determined from the pressure increase in the calibrated permeate volume. The method described in this paper differs substantially from these methods. We measure separately the solubility S the diffusion coefficient D and compute their product. The water vapor permeability of the PEO/PAA multilayer film at 30 °C is exceeding low compared with the 19 polymer membranes in Wessling's Table 1. Only polyethylene and polyvinyl alcohol films have lower permeability. The permeability of a multiblock copolymer of polyethylene oxide and poly(butylene terephthalate) reported by Wessling is 85,500, or almost 2400 times the permeability of the multilayer PEO/PAA film studied here. This surprising result deserves further study.

5. Conclusions

Sorption isotherms, sorption enthalpies, diffusion coefficients, and permeabilities for water in an 11 μm thick PEO/PAA film have been measured at 30, 40, and 60 °C for relative humidities between 0 and 70%. All quantities were measured on the same film using the quartz crystal microbalance/heat conduction calorimeter. Water diffusion coefficients are several orders of magnitude lower than in the separate components. Sorption isotherms are of type III at 30 and 40 °C and linear at 60 °C. The enthalpy of water sorption determined from the sorption isotherms using the van't Hoff relation is 32.9 ± 0.3 kJ/mol. Calorimetric enthalpies of water sorption range from 42 to 34 kJ/mol at 30 and 40 °C over the humidity range studied; the precision of these measurements is not yet sufficient to determine accurate isosteric enthalpies of sorption. The change in motional resistance, a quantity proportion to the loss compliance of the film, has also been recorded at all three temperatures, and a common trend is an increase in loss compliance with increasing relative humidity. This trend has been observed in other polymer systems, and indicates plasticization of the film by water.

Direct calorimetric measurements of water vapor sorption enthalpies are quite uncommon because bulk polymer samples equilibrate slowly with gases and the corresponding rate of heat generation is very low. An advantage to measuring water sorption in thin polymer films is the large surface-to-volume ratio which produces rapid equilibration of the vapor with the polymer. The heat flow from the sample to the thermopile detector and the heat sink occurs in one dimension only, unlike other modes of heat conduction calorimetry, and it occurs on the same time scale as the mass change. With the quartz crystal microbalance, nanogram changes of mass are recorded in real time permitting the determination of diffusion coefficients in thick films such as the one used here. The ability to monitor simultaneously the heat flow, the mass change, and the viscoelastic loss in the same sample is a powerful new capability for characterizing the interaction of thin polymer films with gases and solvent vapors.

References

[1] W.J. Koros, M.R. Coleman, D.R.B. Walker, Annu. Rev. Mater. Sci. 22 (1992) 47.
[2] M.A. Hickner, H. Ghassemi, Y.S. Kim, B.R. Einsla, J.E. McGrath, Chem. Rev. 104 (2004) 4587.
[3] O. Rodriguez, F. Fornasiero, A. Arce, C.J. Radke, J.M. Prausnitz, Polymer 44 (2003) 6323.
[4] A.V. Anantaraman, C.L. Gardner, J. Electroanal. Chem. 414 (1996) 115.
[5] T.A. Zawodzinski, C. Derouin, S. Radzinski, R.J. Sherman, V.T. Smith, T.E. Springer, S. Gottesfeld, J. Electrochem. Soc. 140 (1993) 1041.
[6] Q.G. Yan, H. Toghiani, J.X. Wu, J. Power Sources 158 (2006) 316.

[7] T.R. Farhat, P.T. Hammond, Adv. Funct. Mater. 15 (2005) 945.
[8] D.W. Van Krevelen, in: D.W. Van Krevelen (Ed.), Properties of Polymers, Elsevier, New York, 1990, p. 535.
[9] A.L. Smith, S.R. Mulligan, H.M. Shirazi, J. Polym. Sci. Part B: Polym. Phys. 42 (2004) 3893.
[10] A.L. Smith, New Developments in Coating Technology, in: P. Zarras, B. Richey, T. Wood, B. Benicewicz (Eds.), ACS Symposium Series, Washington, DC, 2006.
[11] A.L. Smith, H.M. Shirazi, Thermochim. Acta 432 (2005) 202.
[12] P. Hernandez-Munoz, R. Gavara, R.J. Hernandez, J. Membr. Sci. 154 (1999) 195.
[13] R. Paterson, Y.P. Yampol'skii, P.G.T. Fogg, J. Phys. Chem. Ref. Data 28 (1999) 1255.
[14] A.L. Smith, H.M. Shirazi, J. Ther. Anal. Calorimetry 59 (2000) 171.
[15] A. Arce, F. Fornasiero, O. Rodriguez, C.J. Radke, J.M. Prausnitz, Phys. Chem. Chem. Phys. 6 (2004) 103.
[16] A. Elberaiche, A. Daro, C. David, Eur. Polym. J. 35 (1999) 1217.
[17] S.J. Metz, W.J.C. van de Ven, M.H.V. Mulder, M. Wessling, J. Membr. Sci. 266 (2005) 51.
[18] M.-J. Chang, A.S. Myerson, T.K. Kwei, J. Appl. Polym. Sci. 66 (1997) 279.
[19] J. Kroschwitz, Concise Encyclopedia of Polymer Science and Engineering, John Wiley & Sons, New York, 1990.
[20] S.J. Metz, W.J.C. van de Ven, J. Potreck, M.H.V. Mulder, M. Wessling, J. Membr. Sci. 251 (2005) 29.
[21] S.-W. Lee, W.D. Hinsberg, K.K. Kanazawa, Anal. Chem. 74 (2002) 125.
[22] R. Lucklum, P. Hauptmann, Faraday Discussion 107 (1997) 123.
[23] A. Katz, M.D. Ward, J. Appl. Phys. 80 (1996) 4153.